Identification and prediction of acute intracranial hemorrhage by using CNN and RNN techniques

D. Sreelakshmi ✉; Syed Inthiyaz; L. V. Narasimha Prasad; Ahmed R. Hassan; Mohammed J. Hussein; Noor Abbas

Check for updates

View Online

Export Citation

Identification and Prediction of Acute Intracranial Hemorrhage by Using CNN and RNN Techniques

D. Sreelakshmi[1, a)], Syed Inthiyaz[2, b)], L. V. Narasimha Prasad[1, c)], Ahmed R. Hassan[3, d)], Mohammed J. Hussein[4, e)] and Noor Abbas[5, f)]

[1] *Institute of Aeronautical Engineering, Hyderabad, Andhra Pradesh, India.*
[2] *Koneru Lakshmi Education Foundation Green Fields, Andhra Pradesh, India.*
[3] *National University of Science and Technology, Dhi Qar, Iraq.*
[4] *Al-Esraa University College, Baghdad, Iraq.*
[5] *Ashur University College, Baghdad, Iraq.*

[a)] *Corresponding author: d.sreelakshmi@iare.ac.in*
[b)] *syedinthiyaz@kluniversity.in*
[c)] *lvnprasad@iare.ac.in*
[d)] *ahmed.r.hassan@nust.edu.iq*
[e)] *mohamed.jabar@esraa.edu.iq*
[f)] *noor.abbas@au.edu.iq*

Abstract. Computed tomography (CT) of the head is utilized worldwide to analyze neurologic crises. Brain hemorrhage could be an extreme danger symptom to human life, and it's convenient and adjust conclusion and treatment has extraordinary significance. Depending on the location and nature of the bleeding, there are many types of a brain hemorrhage. Subdural, epidural, intracranial, intraparenchymal, and subarachnoid hemorrhage are the five most common forms of bleeding. To better understand the types of cerebral bleeding seen in CT scans of the head, this research proposes a new method. Hybrid deep learning representations of convolution neural networks and recursive neural networks are used to classify hemorrhages' (CNN-RNN). For ICH detection and subtype classification, CNN-RNN deep learning is upgraded. This system is fast and exact in ICH identification.

Keywords: CT Scans, Hemorrhage, Deep Learning, Convolutional Neural Network.

INTRODUCTION

Intracranial Hemorrhage (IH) happens when an infected vein inside the mind explodes, permitting blood to leak inside the cerebrum. The abrupt expansion in pressure inside the cerebrum can make harm the mind cells surrounding the blood. Fast expansion in blood sum may cause unexpected development in pressure which thusly can lead to obviousness or passing. IH may stretch out into ventricles in relationship with profound, huge hematomas. Intracranial drain generally happens in chosen portions of the mind, including the basal ganglia, cerebellum, brain stem, or cortex. Intracranial discharge represents 10 to 15 percent of all instances of stroke and is related with the most noteworthy death rate, with just 38% of affected patients enduring the initial year.1, 2IH can be ordered into intra pivotal and extra hub drain dependent on draining inside or outside the cerebrum substance. Intra hub drain can be further classified into cerebral discharge, and intraventricular discharge (IVH) in view of the specific anatomical area of dying. Additional crucial discharge is classier as per the anatomical layer of meninges where draining happens, specifically extra Dural drain (EDH), subdural drain (SDH), subarachnoid discharge (SAH).In moderate to serious head injury cases, non-contrast-improved CT examining is the most valuable and preferred choice for starting imaging method [1][2].

Explanations for this decision are CT examines being fast and its capacity to identify intense discharge, cerebral

growing, proof of raised intracranial pressing factor and pneumocephalus. New intracerebral blood ordinarily seems hyperdense on CT because of the great protein focus and its high mass thickness. Nonetheless, periodically intense intracerebral hematoma can seem is odense or even hypodense on CT [3][4].

CT examining can show the size and area of the Intracranial Hemorrhage precisely. Likewise it can recommend potential causes like tumor, vascular abnormality, or aneurysm.1Since recent years, PC helped finding (CAD) has gotten one of the significant exploration regions in clinical imaging and symptomatic radiology[5][6]. The fundamental idea of CAD is to give a PC yield as a subsequent assessment to help radiologist's picture readings. The objective of CAD is to improve the quality and usefulness of radiologist's [7]

Traumatic brain injury (TBI) is a primary cause of death and permanent disability in the United States of America. Almost three-quarters of all deaths were caused by distracted driving. TBI may lead to intracranial haemorrhage (ICH), which is an extra-axial intracranial lesion (TBI). There is a substantial mortality rate [8] associated with ICH, making it a potentially lethal disease. Due to the seriousness of a secondary brain injury, it is considered to be clinically significant and should be treated accordingly. The five subtypes of ICH include intraventricular (IVH), intraparenchymal (IPH), subarachnoid (SAH), epidural (EDH), and subdural (SDH) depending on their location in the brain (SDH). The medical name for ICH that occurs inside the brain tissue is known as "intracerebral haemorrhage," or "ICH."

Emergency examination of patients with TBI for ICH is often performed with a CT scan (computerised tomography) [9]. For the first examination of ICH, CT scanning is favoured over MRI because of its accessibility and speed of acquisition. Images of brain tissues are captured at different intensities depending on the level of tissue X-ray absorption in a CT scan, which uses X-ray beams (HU). CT images are shown via windowing. The HU numbers are converted into grayscale values according on the window's level and width ([0, 255]). With a variety of window settings (e.g., brain, stroke, and bone), the grayscale image depicts various elements of the brain tissues [10]. It's hard to see exactly what the ICH areas look like in the CT scan images that are shown via the brain window. In order to evaluate whether or not ICH has occurred, as well as the kind and area of the ICH seen on these CT pictures, an experienced radiologist examines them. A subspecialty-trained neuroradiologist must be available for this diagnosis, which means it might be time consuming and potentially erroneous in rural places with limited access to expert treatment [11].

Multiple picture classification and segmentation tasks may now be automated using convolutional neural networks (CNNs), thanks to recent breakthroughs in this technology [5]. Because of this, we believed that deep learning techniques may be used to automate the process of detecting and segmenting ICHs in the future. Each CT slice was segmented using a fully convolutional neural network (FCNN), called as U-Net [12]. Junior radiology trainees might benefit from an automated ICH detection and categorization tool when specialists are not immediately accessible in emergency departments, particularly in poor nations or isolated places. The use of a diagnostic tool like this may considerably minimize the performance time and fault involved diagonalizes of ICH [13][14].

ICH classification has two publicly accessible datasets; however segmentation of this classification technique lacks a publicly accessible dataset. Over 25k CT scans were submitted to Kaggle in September 2019 for the CQ500 dataset, which contains 491 head CT images. A request for data from Arbabshirani et al. or Lee et al. is appreciated. In addition to ICH detection and classification, several research have recommended ICH segmentation. However, several of these strategies were not evaluated due to a lack of public or private datasets with ICH masks [10–14], while others were tested on private datasets with diverse parameters, such as the number of CT scans and the diagnosed ICH types. Because of these differences, it is hard to compare the different approaches with any degree of objectivity. As a result, a dataset for ICH segmentation benchmarking and expansion is required. As a result, the study's major objective was to collect and freely distribute head CT images with ICH segmentation. A complete assessment of the literature on the detection and segmentation of ICH was also carried out. Table 1 lists our contributions to filling the knowledge gap [15][16].

TABLE 1. Contributions of this paper.

Gap in Knowledge	Our Contribution
Publicly available dataset for ICH Segmentation	We collected a ICH dataset and made it publicly available at the physionet repopsitory
Precise ICH Segmentation method	We developed a proof-of-concept ICH segmentation based on U-Net
Literature Review	We review many papers in the ICH detection, classification, and segmentation

RELATED WORK

Nguyen et al. displayed a complete investigation of state-of-the-art on later improvement and disputes of human discovery for illustration acknowledgment, approach exploiting reflective CNN has been emerged to realize customary finishing on numerous picture appreciation seat marks. Dissimilar CNN models for protest location by its protest localization is projected in terms of arrange engineering, calculations, and unused thoughts. In later a long time, CNN models such as Alex Net Therefore, the real-time calculations of question discovery utilizing the CNN demonstrate like R-CNN and YOLO [17]

There has been a lot of fascinating work done to automate the ICH diagnostic process. There has been a lot of work done on detecting ICH sub-types using a two-class detection problem or a multi-class classification problem that involves detecting ICH presence [18]. Researchers have gone a step further and used ICH segmentation to zero down on the exact location of the ICH. Most researchers employed small datasets to validate and test their algorithms, but a handful used big datasets. A complete overview of detection, classification, and segmentation of ICH is presented in this article and its block diagram is shown in figure 1 below.
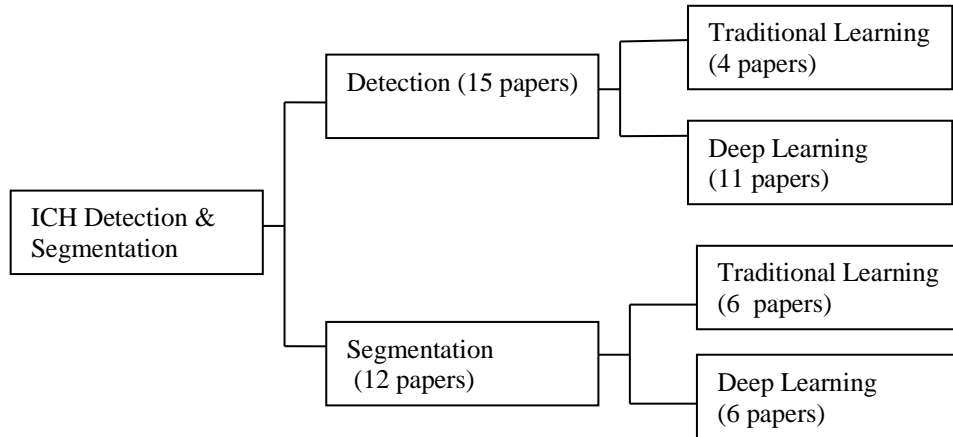
FIGURE 1. Various review papers distribution for ICH procedure

The ICH Classification and Detection

One may find numerous classic and DL methods in the related work. Conventional ML approaches, such as the threshold-based algorithm established by Yuh et al., were used to identify ICH. According to the approach [10], the ICH sub-types may be identified by their size, shape, and position. The authors used a retrospective sample of 33 CT images to refine the threshold value and then tested its methods on 210 CT scans of patients with supposed TBI. For the identification of ICH, their system was 98% sensitive and 59% specific, with an intermediate accuracy in identifying the subtypes. According to Li et al., in a separate research, two methods for segmenting the SAH space and using the segmented parts to detect SAH bleeding were described. One technique used elastic registration with the SAH space atlas, while the other method extracted distance transform characteristics and trained a Bayesian

decision algorithm for the delineation of the region of interest. SAH haemorrhage detection support vector machine classifiers were trained using this data after the SAH space segmentation was done. Algorithms were trained on 60 CT pictures while the model was tested on 69 CT scans (30 with SAH hemorrhage). Decisions made using the Bayesian method have a sensitivity and specificity of 100 percent, as well as a correctness of ninety-one percent [19].

All of the DL approaches were based on CNNs and variants, save those in, which were based on an FCN model. An RNN or random forest model was utilised to account for the spatial dependence between adjacent slices when using these approaches. Sometimes, authors use an interpolation layer or alter CNNs to analyse part or all of a CT scan. A 1-stage technique, on the other hand, ignores the spatial connection between slices. Two CNN-based algorithms were suggested by Prevedello et al. ICH, mass effect, and hydrocephalus were the emphasis of one of their algorithms, whereas suspected acute infarcts were the subject of their other method [20].

Subtypes of IH, including calvarial breakings, midline shift, and mass effect, were identified by Chilamkurthy et al. using four methods. There were more than 280,000 CT images in the dataset used by the researchers to train and test their algorithms. The tests were conducted on two different sets of data. One of them included 491 scans, all of which were made accessible to the public (called CQ500). CT scan training and validation were labelled using clinical radiology reports as the gold standard. Using a natural language processing method, these reports were utilised to categorise each scan. As a final step, the testing scans were interpreted by the three experienced radiologists who reported on the ICH sub-types. For each of the four types of detection, a unique deep model was created. The output layers of ResNet18 were trained using five parallel fully connected layers. A random forest technique was used to forecast the scan-level confidence in the existence of an ICH based on the findings of these resultant layers for every slice. Their average AUC for ICH sub-type categorization was 0.93 across both datasets, according to the study's authors. For comparison, radiologists had an accuracy rate of 92%, based on a high sensitivity operating point. In contrast, the gold standard had a specificity of 95%, but this study's average specificity was 70%. ICH sub-types also had diverse results. SDH detection had the lowest specificity, at 68% [21].

The detection of ICH has been suggested using two CNN-based RNN techniquesGrewal et al. proposed DenseNet, a 40-layer CNN with a bidirectional long short-term memory (LSTM) layer. A total of three auxiliary tasks were added after each dense convolutional block in order to compute binary segmentation of the ICH regions for analysis. Upsampling of the feature maps to their original size was achieved via the use of convolution and deconvolution techniques. The LSTM layer contained the inter-slice dependencies of each subject's CT images. A total of 0365 CT images were utilized for training, 067 CT scans were used for validation, and 077 CT scans were used for testing... By rotating and horizontally flipping the training data, we were able to equalize the number of scans for the two groups. CT slices were annotated by three radiologists and compared to the network detection. With 81.0 percent accuracy, they had an F1 score of 084%; they also had 88% recall (sensitivity). The model's F1 rating was higher than two of the three radiologists' F1 evaluations. With the inclusion of attention layers, the model's sensitivity was considerably enhanced. Researchers employed CNN-RNNs (convolutional and recurrent neural networks) in order to detect and categorize ICH regions. The overall design of this model was similar to that of Grewal and colleagues. Both the CNN and RNN models used bidirectional Gated Recurrent Units (GRUs) (GRU). Slice interpolation was presented by Lee et al. that was comparable to RNNs, but it was more adjustable in terms of the number of adjacent slices used in the classification. The system was ready for deployment after training and testing on 02,537 CT scans [22]. Using a sensitivity and specificity of 099 percent and an AUC of 1, they detected an ICH at the identical slice level. This study's findings were even worse when it came to categorizing ICH subtypes; the overall accuracy was just 093.0%, with an AUC of only 00.93. The least sensitive subtypes were SAH and EDH, both with a sensitivity of 069%.

The CNN model was tweaked in three different ways to handle several CT slices at once. It took Jnawalia et al. three different CNN models to produce an ensemble that could diagnose ICH. AlexNet and GoogleNet were extended to a 3D model by gathering all the slices from each CT scan, and these CNN models were created on top of it. They have fewer parameters since they have fewer layers and filter specifications. They used a huge dataset of 40,000 CT scans to develop, validate, and test their model. A total of 34,000 CT images (26,000 normal scans) were utilised in the training process. We don't know how the CT scans were labelled; that information was omitted. To provide a more balanced dataset for training, only the positive slices were used. Validation and testing required around 2000 and 4000 scans, respectively. Overall Accuracy (AUC), Precision (80%), Recall (77%) and F1-Score (78%) were all over 80% for the CNN models in the ensemble. However, a method by Chang et al. does not incorporate IVH, which may be used to segregate and quantify the amount of ICH zones. In order to generate segmentation masks for ICHs, researchers devised an algorithm that examines parts of five CT scans for ICHs. The researchers trained their system on 10,000.00 CT images, and then tested it on a dataset of 862 CT scans. AUC of

00.97, 095% sensitivity, and an average Dice score of 00.85 were the results of their research, which categorizes ICH subtypes and ICH segmentation. A 00.77 Dice score and a 90.0 percent sensitivity rate were reported for SAH." More than 94,000 CT scans were used to evaluate an ensemble of four 3D CNN models with 24-256-512 512 input shapes, according to Arbabshirani & colleagues (9499 retrospective and 0347 prospective). An AUC of 0.846 was obtained from the retrospective study, with sensitivity and specificity of 071.5 percent and 83.5 percent on both datasets evaluated, respectively [23].

On an ensemble of four well-known CNN models, Lee et al. used transfer learning to identify subtypes of ICH, like Jnawalia et al. ResNet-50, Inception-v3, VGG-16, and Inception-ResNet were the four models. To account for the spatial dependency between adjacent slices, a slice interpolation method was used as well. To train and validate this ensemble model, a total of 904 CT scans were employed, as well as 0200 CT scans and 237 scans for testing. With an AUC of 00.98 and sensitivity and specificity averages of 95.00%, the ICH detection method is very effective. The algorithm, on the other hand, has a 78.3 percent sensitivity and a 092.9 percent specificity for ICH subtype identification. The EDH slices had the lowest sensitivity of 058.3% in the retrospective test set while the IPH slices had the highest sensitivity of 068.8% in the prospective test set. Models fragmentation and radiologists' bleeding-spot maps had 78.10 percent accuracy in localizing the attention maps [24].

ICH Segmentation

To determine the proper medical and surgical treatment, it is necessary to locate and determine the volume of the ICH. Automating the ICH segmentation process has been suggested using many approaches. DL techniques can be used to delineate the boundaries of an ICH, much as ICH detection methods may be used to identify an ICH. CT images must typically be preprocessed to eliminate skull material and background noise in the conventional manner. Additionally, we must register the brain segments and extract a number of technical characteristics. Unsupervised clustering is used in several of these approaches.

Prakash et al. and Shahangian et al. employ the Distance Regularized Level Set Evolution (DRLSE) technique to adapt active contours to ICH regions. Using DRLSE, Prakash et al. modified the preprocessing of the CT images to remove the skull and filter out noise, and then segmented the IVH and IPH sections. The method's Dice coefficient was 0.88, with a sensitivity of 709% and a specificity of 099.9 percent, based on 050 CT scans. The EDH, IPH, and SDH areas were segmented using DRLSE, and the ICH slices were classified using a supervised technique based on support vector machines given by Shahangian et al. [18]. The skull and brain ventricles were removed as the initial stage in their approach. Next, they used DRLSE to segment the ICH. The ICH areas' shape and texture were then extracted, and the ICH was detected as a result of the results of that process. A Dice coefficient of 058.5 was obtained, as well as an 80% sensitivity and a 90.0% specificity on 0627 CT slices using this method. When doing typical unsupervised studies, they used fuzzy c-means clustering. Bhadauria and colleagues proposed a method based on a spatial fuzzy c-means clustering and a region-based active contour model. Twenty CT scans with ICHs were used in the investigation, which was conducted retrospectively. 0The researchers discovered an average Jaccard index of 00.78, with a sensitivity of 79% and a specificity of 100%. This is comparable to the Gautam et al. white matter fuzzy c-means clustering and wavelet-based thresholding technique. Twenty CT images with an ICH were evaluated, and the dice coefficient was 00.82 [25].

Unsupervised approaches, on the other hand, do not use labeled slices to train classifiers. For each CT slice, Chan et al. proposed first segmenting and aligning the brain. A top-hat transformation and extraction of the asymmetrically high-intensity areas were then utilised to identify the ICH regions of interest. An ICH classifier based on prior information was then used to narrow down the list of possible candidates. The sensitivity, specificity, and sensitivity at the lesion level were all 082.6 percent using this method.

One method that was developed by Muschelli et al. was totally automated. There are a number of well-known methods for fragmenting intracranial hemorrhage. CT brain-extracted template was used to extract the brain from the CT picture and register it, as seen in the figure below

Next, a variety of variables related to each scan were examined. Within-plane standard scores and initial categorization using an un - supervised prototype, contra lateral differential visuals, distance to the brain's center, and standardized-to-template intensity that contrasts one CT scan with an averaged CT scan from healthy subjects were included in addition to CT voxel intensity and local moment details such as mean and standard deviation (STD). For categorization, we employed logistic regression, a generalized additive model, and a random forest. A total of 0102 CT scans were utilized to train and test these models. A random forest was used to get the highest Dice coefficient of 00.899.

It was either CNNs or the FCNs architecture that was used for the deep learning algorithms for ICH segmentation (see to references 9, 21, 22 and 23). CNN-based ICH segmentation was discussed in the preceding part [26] [27]. In another study, Nag et al. used a trained autoencoder to pick CT slices having ICHs, and then the active contour Chan-Vese model to segment the ICH regions [28]. The approach was tested on a dataset of 48 CT-Scan images [29].

Only half of the data were used to train the autoencoder, whereas the whole dataset was utilised to test the method. The sensitivity was 71%, the +ve analytical assessment was 73.0%, and the Jaccard index was 00.55 in this study [30].

METHODOLOGY

In the Machine Learning (ML) stage the component-rich pictures are feed into the preparation set. For the execution reason, we have utilized the Keras library in python to run the ML calculation. ML is enlivened by the working of the cerebrum. The entire model comprises of layers, very much like neurons in the cerebrum. This model learns by thinking about models. The consecutive model is made utilizing Keras. At first two layers are added with a rectifier work. The subsequent stage is adding a pooling layer of 2x2 frameworks. Presently the pooled pictures are changed over into a consistent vector.
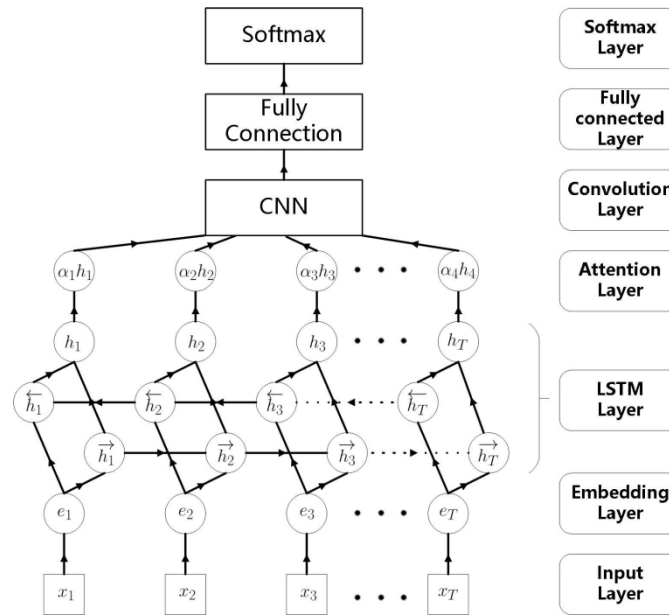

FIGURE 2. Pipeline for proposed model

The secret layer is currently added, this layer will contain every one of the hubs, called counterfeit neurons. These layers mimic the human mind by learning layers by layers. When every one of the layers are added, the model is incorporated and saved as an h5 document which can be stacked toward the front so we don't need to prepare the model without fail.

IMPLEMENTATION

The information gathered comprises of around 1470 records and 35 characteristics and target property that is Attrition of a worker. To anticipate the wearing down of a worker we need to assemble an ML model. For that we have utilized the Jupyter Notebook and IBM cloud for preparing the model and conveying it. Building an ML incorporates the accompanying advances.

a. Pre-processing of data
b. Data feature extraction
c. Data model trainig
d. Prediction
e. Deployment to Prediction

Data Preprocessing

Here data preprocessing consists of 5 different type of CNN layers such as LSTM, Convo (Convo + ReLU), input, pooling, and fully connected (FC) and output layers
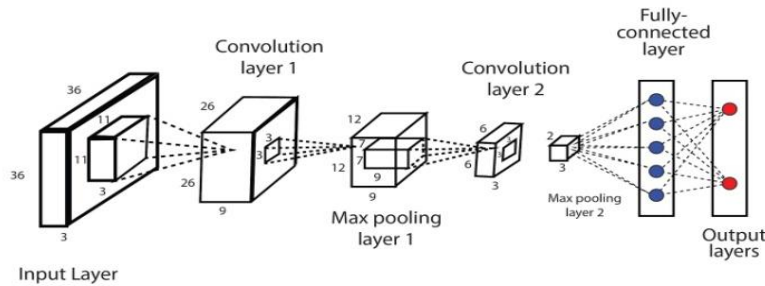
FIGURE 3. Different layers in CNN

CNN's Input Layer

It is essential that CNN's data layers include images. As previously shown, a D3 grid is used to organize picture data. It's not just a single portion that has to be reshaped; the whole thing needs. Take $028 \times 028 = 0784$ as an example; before putting it into input you will need to resize the image by one unit to make it 0784 x 01. Assuming you've been "m" creating model measurements of data (0784, m).

CNN's Convolutional Layer

Because it removes the image's highlights, the Convo layer is also referred to as the Feature extractor layer. To begin with, a portion of the image is linked to the Convo layer, allowing us to do the convolution activity we saw before and determine the spot item among the responsive field and the channel. The yield volume is a single whole number as a result of the activity. Once we've done that, we'll take a step back and do a similar action on the next open field with a comparable information picture. We'll go through the same motions again and again until we've covered the whole image. The next layer's contribution is the results.

CNN's Pooling Layer

To reduce the spatial volume of the information image behind convolution, the pooling layer is used. It is used in conjunction with two convolution layers. In the case that relates FC after the Convo layer without relevant pooling or maximum pooling, then it is computationally expensive and does not require it. As a result, the ideal way to reduce the spatial volume of an information picture is to use the highest amount of pooling possible. Max pooling in a single depth cut through Stride of 2 was employed in the beyond the model. The 4×4 measurement input has been reduced to 2 x 2 measures, as can be seen.

However, there are only two hyperparameters in the pooling layer – Filter(F) and Stride(S).

All things considered, if the input measurement is W1 x H1 x D1, then it's a good bet.

$$W2 = \frac{W1 - F}{S} + 1$$

$$H2 = \frac{H1 - F}{S} + 1$$

$$D2 = D1$$

Where W2, H2 and D2 are the width, Length and profundity of output.

CNN's LSTM Layer

LSTM is a simulated RNN devises uses within the field of deep knowledge. LSTM systems are well-suited to categorizing, arranging and manufacturing forecasts based on time arrangement data, as there are slacks of obscure term among imperative instance in a time series.

Fully Connected Layers (FCL)

Loads, inclinations, and neurons make up FCL. It connects neurons in one layer to neurons in another layer by way of connections. It is used to prepare a range of classes of images and then group them together.

CNN's Softmax / Logistic Layer

The last CNN layer is called Softmax or Logistic. It lingers towards the FC layer's end. Parallel ordering is handled by calculated, while multi-arrangement is handled by softmax.

CNN's Output Layer

As an output, you'll see the name of the layer you're working on and any linked layers like weights, preferences, and neurons. Using this technology, neurons in one layer may communicate with neurons in a second layer. It is used to sort images into several groups using a formula.

CNN's Softmax / Calculated Layer

The last layer of CNN is Softmax or Calculation. Located towards the end of the FC tier, its Double categorization is handled by calculating and multi-categorization by softmax.

CNN's Output Layer

The output layer contains the name encoded in a one-hot format.

Data Preparation

High-quality information has continuously been the essential necessity of learning solid calculations. Especially, preparing a profound neural arrange requires expansive sum of labeled information. Subsequently, high-quality skin infection information with dependable analyze is important for the improvement of progressed calculations. 3 main sorts of models are used for derm illness determination, i.e., clinical pictures, dermoscopy pictures and obsessive pictures. Since clinical pictures of skin injuries are as a rule attain by portable cameras for farther examination taken as therapeutic report for patients.

Dermoscopy pictures are gotten by higher-resolved advanced single-lens reflex (DSLR) or savvy mobile camera connections. Obsessive pictures, attained by checking a tissue slide by a magnifying instrument and digitalized as an picture, are provide as a gold customary for skin illness conclusion. As of late, numerous open datasets for skin malady conclusion errands have begun to emerge. There exists developing drift within the inquire about community to list these datasets for indication. Within the taking after, we display a few freely accessible datasets for skin disease.
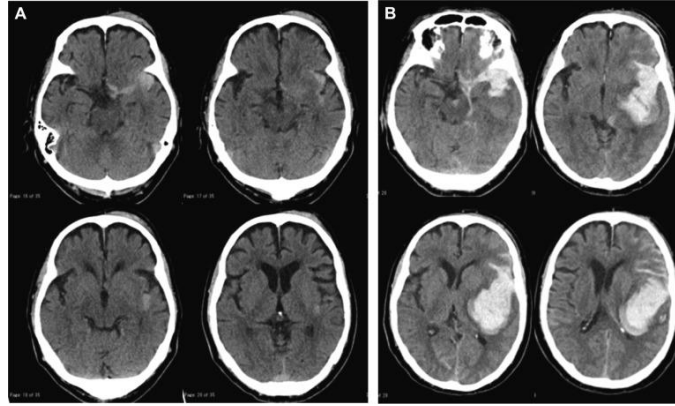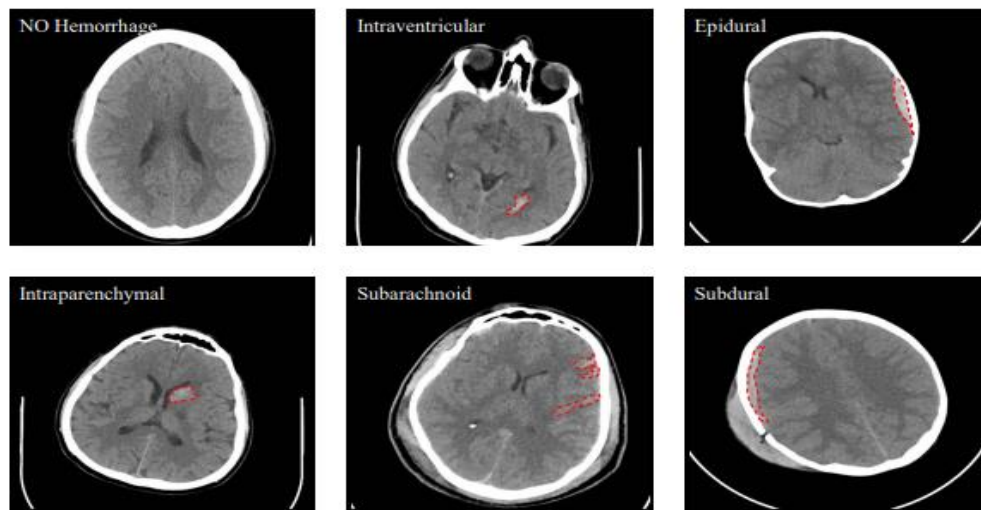
FIGURE 4. Hemorrhage images

FIGURE 5. Sample datasets shows different ICH.

RNN

RNN is a kind of NN wherever that acquiesces by past step is encouraged as input to the current step. In CN systems, all the inputs and give ups are autonomous of each other, but in cases like whenever mandatory to anticipate another word of a ruling, the past words are mandatory and subsequently to keep in mind the past words of RNN approach by the occurrence of settled problem with the help of a Covered up Layer. The most and most unmistakable highlight of RNN is covered up state, that recalls a few data approximately a arrangement.

RNN has a "memory" that recalls all data on what it is determined. It exploits similar boundaries for every contribution as it plays out comparable responsibility on every one of the sources of info or covered up layers to generate the yield. This decreases the intricacy of boundaries, in disparity to added neural organizations

RESULTS & DISCUSSION

Accuracy Score

The accuracy can be termed as closeness of measurements in statistical measures, however it is also used in classifications. In classifications accuracy is the percentage of true results among the total amount of cases. And to our model we got an accuracy of about 85% which indicates a good classification accuracy rate.

Skin problem is developing quickly all over the nation. It is one of the foremost common sorts of maladies where a few can be excruciating and a few can cause lethal to human life. Everybody ought to pay consideration towards this disturbing and developing wellbeing issue which is spreading quickly due to various reasons like worldwide warming. To maintain a strategic distance from delay in treatment, we have developed a demonstration which is able classify the disease using picture dataset. The demonstrate employments the profound learning approach to induce prepared for classification. It works on CNN and RNN.
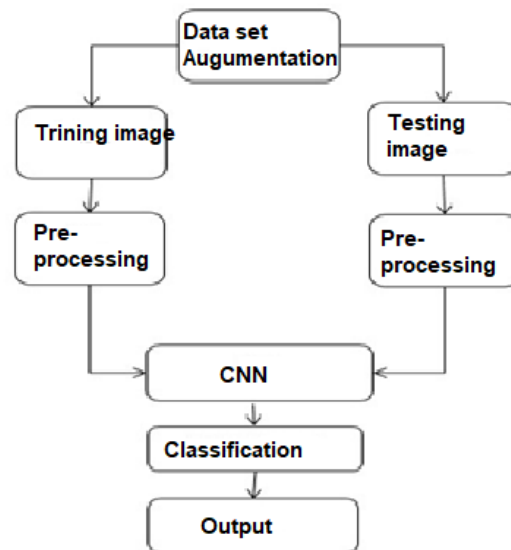

Figure 6. Flowchart for proposed system

There was no pre-processing done on the raw CT slices other than eliminating 5 pixels from the picture borders that were merely black and included no useful information. 640 x 640 CT slices were produced as a consequence of this procedure. We tested U-performance Net's in three different ways and compared it to a threshold-based approach.
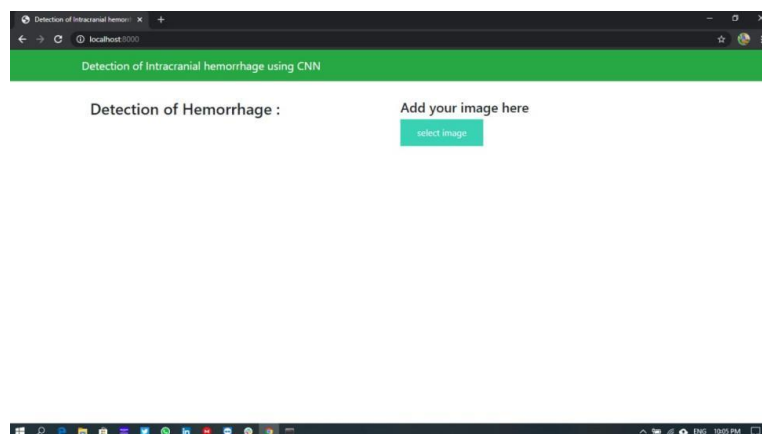

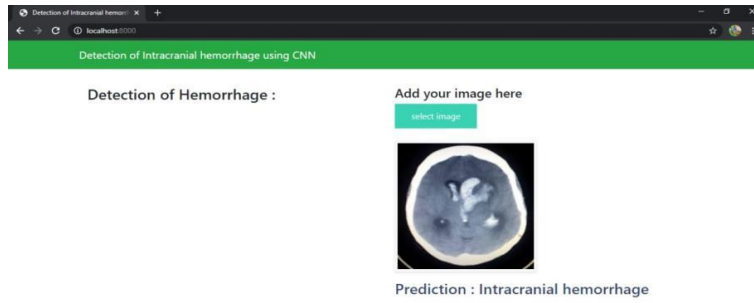**FIGURE 7.** Webpage representation of input image

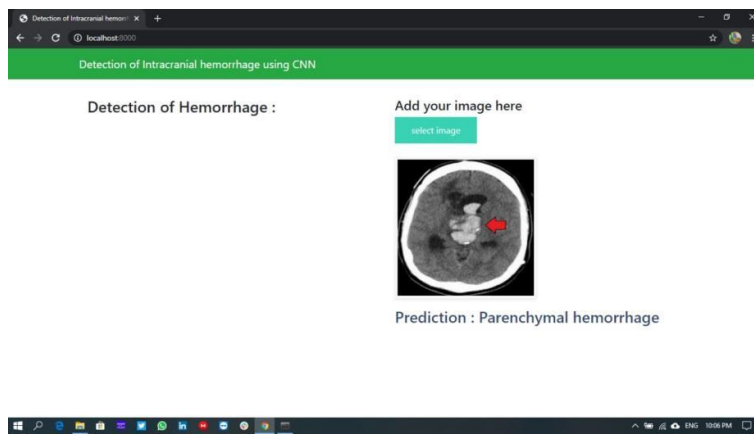**FIGURE 8.** Webpage representation of image prediction

FIGURE 9. Webpage representation of image Hemorrhage

A Dice coefficient of 00.52 was found for SDH segmentation using ICH sub-type data for U-Net. EDH, IVH, IPH, and SAH segments had average Dice scores of 0.35, 0.3, 0.28, and 0.23, respectively. The lowest Dice coefficient and Jaccard index in Table 6 were zero when the U-Net failed to find ICH sites in CT scans of two people. One of the subjects had only a small IPH area in one CT slice, whereas the other had only a little IPH area in two CT slices... IPH zones less than 10mm in width and height constitute the lowest limit of the planned U-ICH Net's segmentation for these individuals. To compare age groups, younger participants' Dice coefficients were found to be 00.321, but older participants' Dice coefficients were found to be only 00.309. People under the age of 018 are not considerably affected by the method's effectiveness, according to this research.

CONCLUSION

The present study investigated a method to identify the Intracranial Hemorrhage using Deep learning algorithm (CNN+RNN) on the image. we propose a way in which the image can be uploaded in an android or ios application and the type of hemorrhage can be detected easily by the person or doctor himself. This can be help full for easier analysis of CT scans.

When an ICH occurs, it is vital to have it checked out as soon as possible, since it may lead to a secondary brain damage that can cause paralysis or even death. The paper's contribution is twofold. New CT scans were acquired, and the results were analysed. As additional publicly accessible benchmark datasets are needed for developing trustworthy ICH segmentation approaches, this dataset has been made available online via PhysioNet. Second, as a proof-of-concept, a deep learning algorithm for ICH segmentation was constructed. Using 5-fold cross-validation on the scanned data, the new strategy was shown to be effective in the real-world. It produced a Dice coefficient of 0.31, which is comparable to the presentation of other DL Algorithms that have been studied and trained on smaller

datasets. It is possible to utilise the U-Net model presented in this work to process CT images. The radiologists may then evaluate the CT scans with the possible ICH spots once they've been processed and cleaned up. Radiologists may use this preprocessing to conduct the final segmentation more efficiently and effectively (in a shorter time). A comprehensive overview of the techniques for detecting, classifying, and segmenting ICHs is also included in the publication.

REFERENCES

1. Singhal, P., Srivastava, P. K., Tiwari, A. K., & Shukla, R. K. (2022). A Survey: Approaches to Facial Detection and Recognition with Machine Learning Techniques. In Proceedings of Second Doctoral Symposium on Computational Intelligence (pp. 103-125). Springer, Singapore.
2. Aggarwal, K., Mijwil, M. M., Al-Mistarehi, A. H., Alomari, S., Gök, M., Alaabdin, A. M. Z., & Abdulrhman, S. H. (2022). Has the Future Started? The Current Growth of Artificial Intelligence, Machine Learning, and Deep Learning. Iraqi Journal For Computer Science and Mathematics, 3(1), 115-123.
3. Shwartz-Ziv, R., & Armon, A. (2022). Tabular data: Deep learning is not all you need. Information Fusion, 81, 84-90.
4. Bhattacharya, S., Somayaji, S. R. K., Gadekallu, T. R., Alazab, M., & Maddikunta, P. K. R. (2022). A review on deep learning for future smart cities. Internet Technology Letters, 5(1), e187.
5. Krizhevsky, A., Sutskever, I., & Hinton, G. E. (2012). Imagenet classification with deep convolutional neural networks. Advances in neural information processing systems, 25, 1097-1105.
6. Deng, J., Dong, W., Socher, R., Li, L. J., Li, K., & Fei-Fei, L. (2009, June). Imagenet: A large-scale hierarchical image database. In 2009 IEEE conference on computer vision and pattern recognition (pp. 248-255). Ieee.
7. Simonyan, K., & Zisserman, A. (2014). Very deep convolutional networks for large-scale image recognition. arXiv preprint arXiv:1409.1556.
8. Szegedy, C., Vanhoucke, V., Ioffe, S., Shlens, J., & Wojna, Z. (2016). Rethinking the inception architecture for computer vision. In Proceedings of the IEEE conference on computer vision and pattern recognition (pp. 2818-2826).
9. He, K., Zhang, X., Ren, S., & Sun, J. (2016). Deep residual learning for image recognition. In Proceedings of the IEEE conference on computer vision and pattern recognition (pp. 770-778).
10. Girshick, R., Donahue, J., Darrell, T., & Malik, J. (2014). Rich feature hierarchies for accurate object detection and semantic segmentation. In Proceedings of the IEEE conference on computer vision and pattern recognition (pp. 580-587).
11. Redmon, J., Divvala, S., Girshick, R., & Farhadi, A. (2016). You only look once: Unified, real-time object detection. In Proceedings of the IEEE conference on computer vision and pattern recognition (pp. 779-788).
12. Ross, G. I. R. S. H. I. C. K., Jeff, D., Trevor, D., & Jitendra, M. (2014, June). Rich feature hierarchies for accurate object detection and semantic segmentation. In Proceedings of the IEEE conference on computer vision and pattern recognition (pp. 580-587).
13. Anupama, C. S. S., Sivaram, M., Lydia, E. L., Gupta, D., & Shankar, K. (2020). Synergic deep learning model–based automated detection and classification of brain intracranial hemorrhage images in wearable networks. Personal and Ubiquitous Computing, 1-10.
14. Patel, A., Van De Leemput, S. C., Prokop, M., Van Ginneken, B., & Manniesing, R. (2019). Image level training and prediction: intracranial hemorrhage identification in 3D non-contrast CT. IEEE Access, 7, 92355-92364.
15. Ye, H., Gao, F., Yin, Y., Guo, D., Zhao, P., Lu, Y., ... & Xia, J. (2019). Precise diagnosis of intracranial hemorrhage and subtypes using a three-dimensional joint convolutional and recurrent neural network. European radiology, 29(11), 6191-6201.
16. Ko, H., Chung, H., Lee, H., & Lee, J. (2020, July). Feasible study on intracranial hemorrhage detection and classification using a CNN-LSTM network. In 2020 42nd Annual International Conference of the IEEE Engineering in Medicine & Biology Society (EMBC) (pp. 1290-1293). IEEE.
17. Nguyen, N. T., Tran, D. Q., Nguyen, N. T., & Nguyen, H. Q. (2020). A CNN-LSTM architecture for detection of intracranial hemorrhage on CT scans. arXiv preprint arXiv:2005.10992.
18. Hssayeni, M. D., Croock, M. S., Salman, A. D., Al-khafaji, H. F., Yahya, Z. A., & Ghoraani, B. (2020). Intracranial hemorrhage segmentation using a deep convolutional model. Data, 5(1), 14.

19. Burduja, M., Ionescu, R. T., & Verga, N. (2020). Accurate and efficient intracranial hemorrhage detection and subtype classification in 3D CT scans with convolutional and long short-term memory neural networks. Sensors, 20(19), 5611.

20. Mansour, R. F., & Aljehane, N. O. (2021). An optimal segmentation with deep learning based inception network model for intracranial hemorrhage diagnosis. Neural Computing and Applications, 1-13.

21. Sreelakshmi, D., & Inthiyaz, S. (2021). A pervasive health care device computing application for brain tumors with machine and deep learning techniques. International Journal of Pervasive Computing and Communications.

22. Sreelakshmi, D., & Inthiyaz, S. (2021). Fast and denoise feature extraction based ADMF–CNN with GBML framework for MRI brain image. International Journal of Speech Technology, 24(2), 529-544.

23. Saikumar, K., Rajesh, V., Babu, B.S. (2022). Heart disease detection based on feature fusion technique with augmented classification using deep learning technology. Traitement du Signal, Vol. 39, No. 1, pp. 31-42. https://doi.org/10.18280/ts.390104

24. Shravani, C., Krishna, G. R., Bollam, H. L., Vatambeti, R., & Saikumar, K. (2022, January). A Novel Approach for Implementing Conventional LBIST by High Execution Microprocessors. In 2022 4th International Conference on Smart Systems and Inventive Technology (ICSSIT) (pp. 804-809). IEEE.

25. Nagendram, S., Nag, M. S. R. K., Ahammad, S. H., Satish, K., & Saikumar, K. (2022, January). Analysis For The System Recommended Books That Are Fetched From The Available Dataset. In 2022 4th International Conference on Smart Systems and Inventive Technology (ICSSIT) (pp. 1801-1804). IEEE.

26. Jothsna, V., Patel, I., Raghu, K., Jahnavi, P., Reddy, K. N., & Saikumar, K. (2021, March). A Fuzzy Expert System for The Drowsiness Detection from Blink Characteristics. In 2021 7th International Conference on Advanced Computing and Communication Systems (ICACCS) (Vol. 1, pp. 1976-1981). IEEE.

27. Appalaraju, V., Rajesh, V., Saikumar, K., Sabitha, P., & Kiran, K. R. (2021, December). Design and Development of Intelligent Voice Personal Assistant using Python. In 2021 3rd International Conference on Advances in Computing, Communication Control and Networking (ICAC3N) (pp. 1650-1654). IEEE.

28. Naidu, T. P., Gopal, K. A., Ahmed, S. R., Revathi, R., Ahammad, S. H., Rajesh, V., ... & Saikumar, K. (2021, December). A Hybridized Model for the Prediction of Heart Disease using ML Algorithms. In 2021 3rd International Conference on Advances in Computing, Communication Control and Networking (ICAC3N) (pp. 256-261). IEEE.

29. Teju, V., Sowmya, K. V., Yuvanika, C., Saikumar, K., & Krishna, T. B. D. S. (2021, December). Detection of Diabetes Melittus, Kidney Disease with ML. In 2021 3rd International Conference on Advances in Computing, Communication Control and Networking (ICAC3N) (pp. 217-222). IEEE.

30. Saikumar, K., Rajesh, V. (2020). A novel implementation heart diagnosis system based on random forest machine learning technique International Journal of Pharmaceutical Research 12, pp. 3904-3916.

31. Shahab S., Agarwal P., Mufti T., Obaid A.J. (2022) SIoT (Social Internet of Things): A Review. In: Fong S., Dey N., Joshi A. (eds) ICT Analysis and Applications. Lecture Notes in Networks and Systems, vol 314. Springer, Singapore. https://doi.org/10.1007/978-981-16-5655-2_28.